X-ray Diffraction Analysis of the Inactivation of Chymotrypsin by 3-Benzyl-6-chloro-2-pyrone†

Dagmar Ringe and James M. Mottonen
Department of Chemistry, Massachusetts Institute of Technology, Cambridge, Massachusetts 02139
Michael H. Gelb and Robert H. Abeles*
Graduate Department of Biochemistry, Brandeis University, Waltham, Massachusetts 02254
Received December 31, 1985; Revised Manuscript Received April 21, 1986

ABSTRACT: The inactivation of chymotrypsin by 3-benzyl-6-chloro-2-pyrone has been studied. A covalent adduct is formed that deacylates slowly with a half-life of 23 h. X-ray diffraction analysis at 1.9-Å resolution of the inactivator–enzyme complex shows that the γ-oxygen of the active-site serine (serine-195) is covalently attached to C-1 of (*Z*)-2-benzylpentenedioic acid, the benzyl group of the inactivator is held in the hydrophobic specificity pocket of the enzyme, and the free carboxylate forms a salt bridge with the active-site histidine (histidine-57). The conformational changes that occur in the protein as a result of complexation are described. It is proposed that formation of the salt bridge prevents access of water and, therefore, hydrolysis of the acyl-enzyme.

We have recently reported that serine proteases are inactivated by substituted 6-chloro-2-pyrones (Westkaemper & Abeles, 1983). The benzyl-substituted chloropyrones **1** and **2** are mechanism-based inactivators of chymotrypsin.

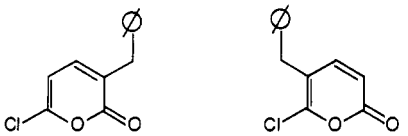

1 **2**

A combination of X-ray diffraction and ^{13}C NMR analyses of the adduct formed between **2** and chymotrypsin showed that the γ-oxygen of the active-site serine (serine-195) becomes covalently attached to carbon-6[1] of the pyrone ring (Scheme I) (Ringe et al., 1985). The binding of the benzyl substituent into the hydrophobic specificity pocket on the enzyme positions the halo-enol carbon of **2** next to serine-195 such that conjugate addition can occur.

Compound **1** contains the benzyl substituent adjacent to the pyrone carbonyl group. In this case, attack of serine-195 occurs at the carbonyl carbon, resulting in the opening of the pyrone ring. Scheme II shows the proposed pathway for the inactivation of chymotrypsin by **1** (Gelb & Abeles, 1984). ^{13}C NMR structural studies (Gelb & Abeles, 1984) of the enzyme-inactivator adduct established that the halo-enol carbon hydrolyses on the enzyme to a carboxylate group, the inactivator is linked to the enzyme via an ester linkage between the carbonyl carbon of **1** and presumably the γ-oxygen of serine-195, and a double bond is located in the α,β-position[2] to this ester linkage. The stereochemical arrangement of the substituents about the double bond (*E* vs. *Z*) had not yet been established.

The acyl-enzyme shown in Scheme II deacylates slowly with a half-time of 23 h (Westkaemper & Abeles, 1983). Concomitant with reactivation (deacylation) (*E*)-4-benzyl-2-pentenedioic acid (**3**) is released (Gelb & Abeles, 1984). It was previously suggested that the C-6-derived carboxylate group was important in the stabilization of the complex since an acyl-enzyme that contains a methyl group in place of the carboxylate group deacylates rapidly (half-time = 4.7 min) (Gelb & Abeles, 1984).

Scheme I: Inactivation of Chymotrypsin by 5-Benzyl-6-chloro-2-pyrone

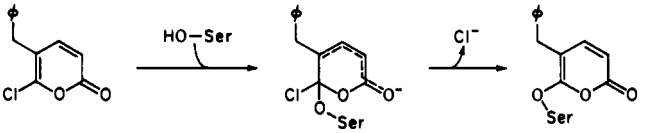

Scheme II: Mechanism of Inactivation of Chymotrypsin by 3-Benzyl-6-chloro-2-pyrone

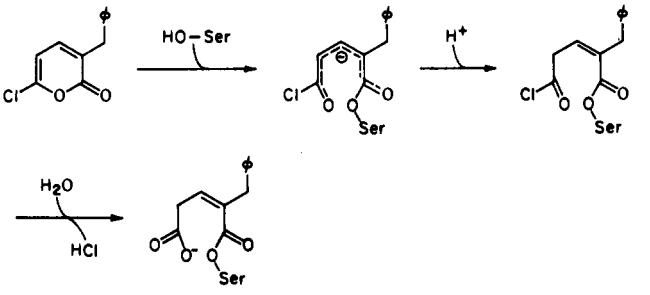

Inactivated Enzyme

In this report, the X-ray structure of the adduct formed between chymotrypsin and **1** is presented. This study was carried out in order to establish the stereochemistry of the substituents about the inactivator double bond, to directly determine the site of covalent attachment to the enzyme, and to provide an explanation, at the molecular level, for the role

† Publication 1590 from the Graduate Department of Biochemistry, Brandeis University. This work was supported in part by NIH Grants 5 R01 GM12633-21 and GM26788-05 and by an American Cancer Society postdoctoral fellowship to M.H.G.

[1] The chloropyrone ring is numbered according to the conventional scheme. The ring oxygen atom is position 1. The ring atoms are numbered consecutively in a counterclockwise manner around the ring.

[2] The α-position of the enzyme-bound inactivator refers to the carbon atom adjacent to the carbonyl carbon of the covalent ester linkage. Thus, the α-carbon is derived from C-3 of the original chloropyrone. The β- and γ-carbon atoms are derived from C-4 and C-5 of the chloropyrone, respectively.

0006-2960/86/0425-5633$01.50/0

of the carboxylate group in the stabilization of the acyl-enzyme.

Materials and Methods

γ-Chymotrypsin crystals were a gift from David R. Davies (NIH). The crystals were stored in 10 mM cacodylate buffer, pH 5.6, containing 75% saturated ammonium sulfate. Compound **1** was prepared as described (Westkaemper & Abeles, 1983).

Crystalline γ-chymotrypsin was inactivated with **1** by soaking individual crystals in 1 mL of a solution containing 10 mM cacodylate buffer, pH 5.6, 75% saturated ammonium sulfate, 5% dioxane, and 0.7 mM inactivator for a minimum of 1 week at 4 °C in the dark. Additional inactivator (50 μL of 13.6 mM **1** in dioxane) was added after 3 days. The final concentration of dioxane was 9% and that of **1** 0.77 mM, assuming no hydrolysis. The enzyme was found to be totally inactive when crystals were redissolved and assayed with benzoyl-L-tyrosine ethyl ester (Hummel, 1959) for catalytic activity. Remaining activity was less than 10%. The inactivated crystals were stored at <−10 °C to prevent deacylation of the complex.

The native crystals belong to space group $P4_22_12$ with unit cell dimensions $a = b = 69.6$ Å, $c = 97.4$ Å, and $\alpha = \beta = \gamma = 90°$ (Segal et al., 1971). The inactivated crystals had unit cell dimensions $a = b = 69.4$ Å, $c = 96.9$ Å, and $\alpha = \beta = \gamma = 90°$, indicating no major changes in the structure of the unit cell.

Data to 1.9-Å resolution were collected on a Nicolet P3 diffractometer equipped with a modified LT-1 low-temperature device. Measurements were made at −15 °C on one crystal using Wyckoff scans to keep radiation damage at less than 25%. Only one crystal was used to avoid trying to scale together data from crystals possibly having different occupancies of the inhibitor. Data were reduced in the usual way (Ringe et al., 1983). A total of 12 800 observed reflections (77% of expected reflections) with intensities greater than 2σ were used to calculate a difference Fourier map by using phases and native amplitudes calculated from the Protein Data Bank coordinates for γ-chymotrypsin (Bernstein et al., 1977). In the calculation of native phases and Fs the active site water molecules and side-chain atoms of Ser-195 and His-57 were omitted to provide an undistorted, unbiased view of the inactivator density, the densities for these two critical residues, and any connection between them. The map showed the bound inhibitor and a number of changes in the positions of residues near the active site. A $2F_o - F_c$ Fourier map displayed on an Evans and Sutherland PS300 computer graphics system was used to build the inactivator structure into the observed electron density and reposition some of the protein residues that had changed position in the inhibited enzyme. The structure initially fitted into the density for the inhibitor had no preconceived geometry applied to the covalent bonds and angles. All carbons, with the exception of the phenyl carbons, were built as sp^3. The structure of the complex was then refined by the restrained least-squares method of Hendrickson and Konnert (1979). In the early refinement cycles no restraints on bond angles or torsion angles were applied to the inhibitor. During this refinement, the structure was rebuilt once from a new $2F_o - F_c$ map, using a computer graphics system, in order to obtain the best fit. During this refitting, it was noted that the phenyl ring remained planar (within 0.07 Å) and the α-position (relative to the ester linkage at Ser-195) also refined to be planar and trigonal. Since this gives an indication of the position of the double bond, the structure having the double bond in the α,β-position was used for further refinement. An attempt was made to fit an alternate structure, having the double bond in the β,γ-position, but this structure could not be made to fit the observed electron density. In total, 25 refinement cycles were used to give a final R factor of 19.1% for all data from 10- to 1.9-Å resolution. The overall B for the final structure was 12 Å^2. The previously reported overall B for the native structure was 11 Å^2 (Cohen et al., 1981). In the final refinement cycles, the occupancies of the inactivator atoms were allowed to vary. The average occupancy calculated was 85%. The restraints applied to the protein (root-mean-square deviation from ideality) and final root-mean-square deviations after refinement are given in Table I.

Table I: Results of Least-Squares Refinement of the Enzyme–Inhibitor Complex

no. of cycles	21
R ($=\sum\|\|F_o\| - \|F_c\|\|/\sum\|F_o\|$)	0.195
no. of reflections (10–1.9 Å)	12800
no. of atoms (non-hydrogen, no solvent)	1751
no. of variable parameters	7005
$\bar{B}$ (Å^2)	
restraints applied	
σ (bond length, Å)	0.025 Å
σ (angle length, Å)	0.030 Å
σ (planar distances, Å)	0.040 Å
deviations observed[a]	
rms Δ (bond length, Å)	0.023 Å
rms Δ (angle length, Å)	0.023 Å
rms Δ (planar distances, Å)	0.036 Å

[a] These Δ values are root-mean-square (rms) deviations from the corresponding values for ideal groups derived from small-molecule structural studies (Sielecki et al., 1979).

Table II: Atomic Coordinates (Å) and Isotropic B Factors (Å^2) for the Enzyme-Bound Inhibitor[a]

atom	x	y	z	B
serine-O$^\gamma$	37.09	76.46	84.93	12
O-1[b]	35.27	77.75	84.64	17
C-1[b]	35.73	76.72	85.11	15
C-2[b]	34.84	75.98	85.96	16
C-3[b]	33.35	75.72	85.25	16
C-4[b]	33.18	76.33	83.74	18
C-5[b]	33.60	75.41	82.93	19
O-5[b]	34.78	74.90	83.07	18
O-5[b]	32.83	74.84	81.89	18
benzylic carbon[c]	35.40	75.49	87.41	15
C-1[1c]	36.53	76.55	87.84	15
C-2[1c]	36.57	76.67	89.22	17
C-3[1c]	37.44	77.45	89.83	17
C-4[1c]	38.34	78.28	89.11	18
C-5[1c]	38.29	78.19	87.86	16
C-6[1c]	37.33	77.36	87.26	16

[a] The coordinates correspond to the system previously defined (Bernstein et al., 1977). [b] Atoms of the pentenedioic acid. [c] Atoms of the benzylic substituent.

Results and Discussion

Description of the Structure of Chymotrypsin Inactivated with **1**. The structure of the bound inactivator fitted to the observed electron density is shown in Figure 1. The refined coordinates and B factors for the non-hydrogen atoms of the bound inactivator are listed in Table II. The inactivator is covalently attached to the enzyme through an ester linkage involving the γ-oxygen of serine-195 and the C-1 carbonyl carbon of the inactivator derived from C-2 of **1**. The observed electron density supports a double bond in the α,β-position to the ester linkage. Attempts to fit a structure having the double bond in the β,γ-position failed to give a fit. This observation is consistent with ^{13}C NMR studies that demonstrated the presence of a double bond adjacent to the ester (Gelb & Abeles, 1984). The stereochemistry of the substituents about

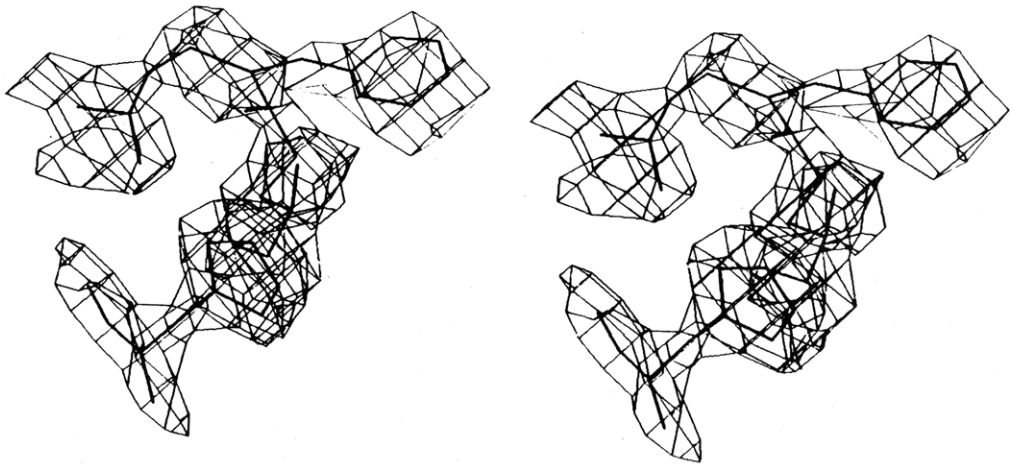

FIGURE 1: Model of the inhibitor fitted to the difference electron density map, $2F_o - F_c$, at 1.9-Å resolution. The electron density corresponding to the bound inhibitor, histidine-57 and serine-195 is shown. Changes in the protein structure as a result of complexation with the inactivator are discussed in the text and presented in Figure 3.

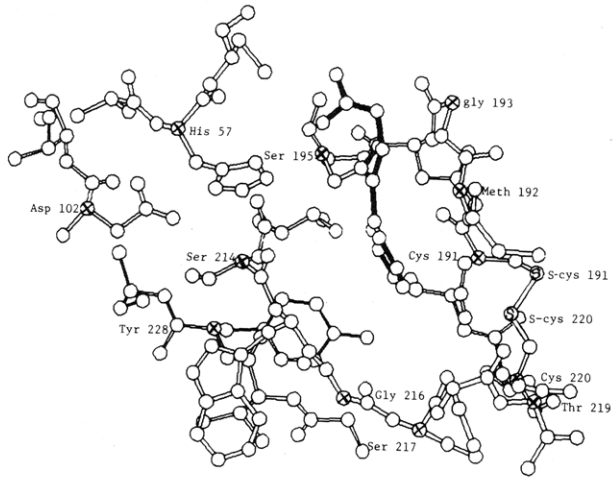

FIGURE 2: View of the active-site region of the enzyme–inhibitor complex. Selected residues have been numbered (labeled) as a guide for the following figures. In each case the α-carbon is indicated (x) plus the two sulfur atoms of the disulfide bridge (S). The inhibitor is indicated in black. The peptide segments from numbers 56 to 58, 102 to 103, 189 to 195, 213 to 220, and 226 to 229 are shown.

the double bond is such that the ester linkage is cis to the carboxymethyl substituent. Thus, the inactivator–enzyme complex is an ester formed between serine-195 and the C-1 carbonyl group of (*Z*)-2-benzylpentenedioic acid.

Figure 2 shows the final refined structure of the inactivated enzyme in the region of the active site. Important residues have been numbered to use as a guide for Figures 3–5. Figure 3 shows the structure of the inactivated enzyme superimposed on the structure of the native enzyme. The structure of the enzyme has undergone some changes as a consequence of the binding of the inactivator (Figure 3). The active-site residues, aspartate-102, histidine-57, and serine-195, have moved in response to the inhibitor. Serine-195 has moved toward histidine-57 by 0.7 Å and rotated about χ_1 by 15°, histidine-57 has moved toward serine-195 by 0.25 Å and has rotated about χ_1 by 21°, and aspartate-102 has rotated about χ_2 by 25°. The net effect of these movements is to close the distance between the serine-195 γ-oxygen and histidine-57 by ~1 Å, while keeping the aspartate-102 to histidine-57 distance constant. The benzyl substituent of the inactivator is bound at the top of the aromatic binding site of the enzyme. The pocket has closed in around the benzyl group. This adjustment can be divided into four main regions: residues 213–216, which comprise one side of the pocket, have moved toward the benzyl group (measured along the α-carbon backbone) by ~0.25 Å; residues 217–219, which lie along the other side of the pocket have moved as much as ~1.5 Å inward; residues 226–229, which lie along the bottom of the pocket, have moved ~0.25 Å. In addition, tyrosine-228 has rotated about χ_1 by 14° to form a close-contact hydrophobic interaction with the benzyl group of the inactivator.

On the basis of the positions of water molecules in the native structure (Cohen et al., 1981), at least six molecules have been displaced by the inhibitor, including the one between histidine-57 and serine-195. The complete water structure for this complex has not yet been determined except in the active-site region.

The structure of chymotrypsin inactivated with **1** shows that the carbonyl oxygen of the acyl linkage to serine-195 is pointing inward toward the interior of the protein. The carbonyl oxygen forms two hydrogen bonds to the backbone amide NHs of residues glycine-193 and serine-195. A similar type of hydrogen bonding network is seen in the structure of Ac-Pro-Ala-Pro-Tyr-OH bound to the serine protease from *Streptomyces griseus* (James et al., 1980). This region of the enzyme, which donates hydrogen bonds to the substrate carbonyl group, has been termed the oxyanion binding site (Robertus et al., 1972) and may play a role in the stabilization of the oxyanion that forms when the substrate carbonyl group becomes tetrahedral. A previous study of the structure of indolylacryloyl-α-chymotrypsin showed that the carbonyl group in this acyl-enzyme is directed away from the oxyanion hole (Henderson, 1970). It was suggested that this misalignment of the carbonyl group is one factor that contributes to the stability of the indolylacryloyl-enzyme derivative. The stability of the acyl-enzyme formed between chymotrypsin and **1** appears not to be due to improper alignment of the acyl linkage.

The refined structure of the enzyme–inhibitor complex has fitted the ester linkage in a slightly nonplanar form (the torsion angle Ser-C^{β}–O^{γ}–inhibitor-C^1-O^1 = −33°). It is possible to reposition the carbonyl oxygen within the electron density for the inhibitor such that this angle has the ideal value of 0°. However, since the refinement has given a best fit slightly different than this value, we have left it. The best fit position still makes the H-bonding interactions that the ideal position also makes.

Perhaps the most interesting observation is the presence of a salt bridge between the inactivator terminal carboxylate group and histidine-57. This is shown in Figure 4. The terminal carboxylate group is 3.4 Å away from one of the

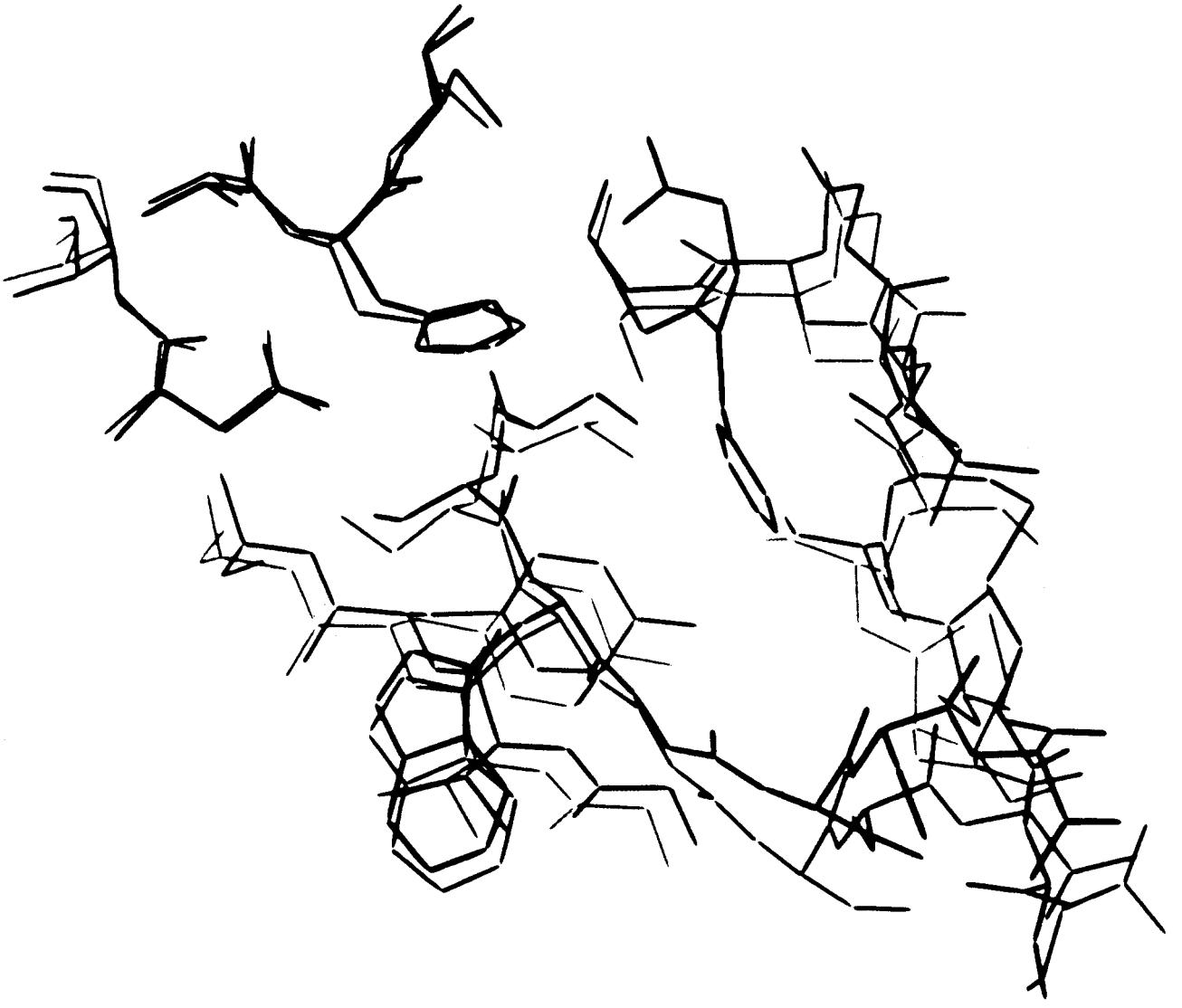

FIGURE 3: Stereoview of the active-site region of the enzyme–inhibitor complex. The structure of the native enzyme (light lines) has been overlayed onto the structure of the enzyme–inhibitor complex (dark lines). Sections of protein that have not changed position significantly appear superimposed.

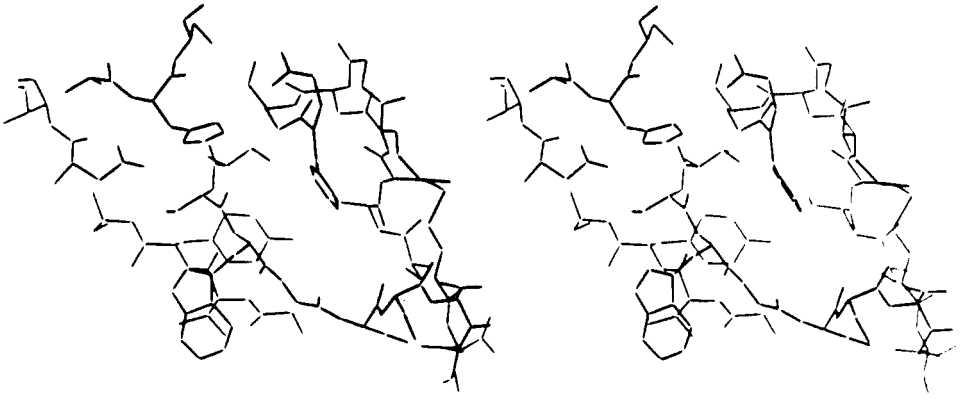

FIGURE 4: Stereoview of the enzyme–inhibitor complex in the region of the active site. The view is the same as in Figures 2 and 3.

nitrogens of histidine-57. Presumably histidine-57 is fully protonated. The other nitrogen of the imidazole ring is hydrogen bonded to aspartate-102. The consequence of this salt bridge, combined with the covalent bond to Ser-195, is that the benzyl substituent of the inactivator has been pulled to the top of the aromatic binding site on the enzyme. In contrast, the structure of chymotrypsin inactivated with the 5-benzyl isomer **2** shows that the benzyl group is bound much deeper in the pocket.

Implication of the X-ray Structure on the Stability of the Acyl-Enzyme and the Process of Reactivation. The reasons for the stability of the acyl-enzyme formed from the inactivation of chymotrypsin by **1** can now be discussed in light of the structural results presented above. The most important result is the observation of a salt bridge formed between the C-6 carboxylate group of the inactivator and histidine-57. This will have at least two effects. First, the salt bridge will sterically prevent a water molecule from hydrogen bonding to

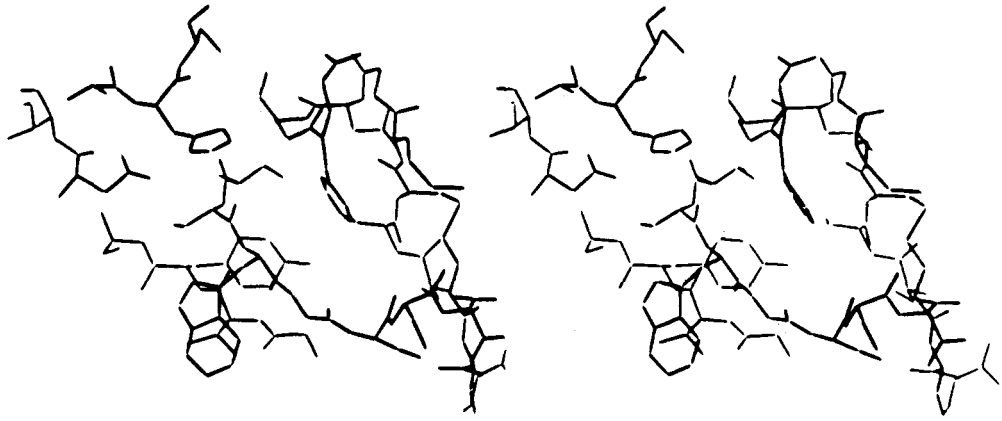

FIGURE 5: Stereoview of the computer-aided model of the γ-chymotrypsin–inactivator complex showing the end carboxylate of the inhibitor rotated away from the enzyme. The carboxylate group has rotated away from histidine-57 about the C_3–C_4 single bond, leaving the imidazole of His-57 exposed to solvent.

histidine-57 in order that it be activated for attack on the serine–acyl linkage. It has been pointed out that the water molecule hydrogen bonded to histidine-57 in the native enzyme has been displaced by the inactivator. Second, the juxtaposition of the negatively charged carboxylate group next to histidine-57 is expected to cause an increase in the pK_a of the imidazole ring. In the native enzyme, histidine-57 has a pK_a of about 6.1 (Markley & Ibanez, 1978). In the complex with **1**, the pK_a is expected to be much higher, so that the imidazole ring will be essentially fully protonated at neutral pH. The result will be a decrease in the ability of histidine-57 to function as a general base in promoting the deacylation of the acyl-enzyme. It is important to point out that the position of histidine-57 has not changed significantly as a result of inactivation by **1** (Figure 3).

Since the structure of the inactivated enzyme is known and the product of the slow reactivation has been identified as (*E*)-4-benzyl-2-pentenedioic acid (**3**) (Gelb & Abeles, 1984), the chemical pathway for reactivation can now be described (Scheme III). Reaction of the chloropyrone with chymotrypsin leads to the formation of a covalent adduct (Scheme III, structure **4**). The detailed reaction sequence leading to this adduct is shown in Scheme II. For the purpose of this discussion, it is important to note that adduct formation involves addition of a solvent proton (H_b) to the γ-carbon. After protonation at the γ-position, the proton (H_a) that was originally present in the chloropyrone now points toward the protein, away from the solvent. The C-6 carboxylate group is held in place by the salt bridge to histidine-57, which effectively blocks access of water to the active site. Occasionally, the carboxylate rotates about the C_3–C_4 bond (Scheme III, structures **4** and **5**). With the model derived from crystallographic analysis, free rotation without interference from the protein can easily occur, placing the carboxylate away from the protein (Figure 5) and positioning the H_a proton toward the solvent. After rotation has occurred, H_a can be abstracted and the double bond can migrate (Scheme III, structures **5** and **6**). Migration of the double bond freezes the carboxylate group into the *E* configuration, far removed from histidine-57. This opens the active site to allow water to enter and hydrolysis of the acyl-enzyme to occur, resulting in reactivation and release of the product **3**.

The mechanism shown in Scheme III is consistent with, and explains, results previously obtained (Gelb & Abeles, 1984). When chymotrypsin is inactivated with [5-^{2}H]-2-chloropyrone, an isotope effect on reactivation (k_H/k_D = 2.5) occurs. These observations imply that the hydrogen that is abstracted during reactivation is not the hydrogen introduced by solvent when

Scheme III: Mechanism of Reactivation of Chymotrypsin Inactivated by 3-Benzyl-6-chloro-2-pyrone

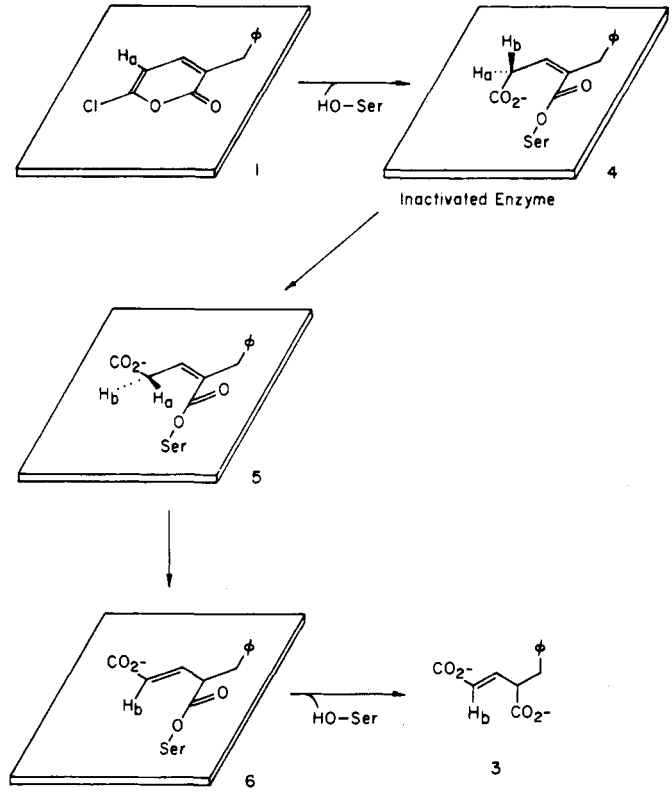

the inactive complex is formed (Scheme III, structure 4). This is in accordance with the reaction sequence shown in Scheme III. When the inactivation is carried out with [5-^{2}H]-2-chloropyrone, the hydrogen designated H_a is ^{2}H. In the inactive complex this hydrogen points toward the protein. When the subsequent rotation (Scheme III, structures **4** and **5**) takes place, H_a points toward the solvent and is abstracted. Hence, an isotope effect on reactivation is observed.

CONCLUSIONS

The results presented in this study characterize the complex formed between **1** and chymotrypsin. The interaction of the benzyl substituent of **1** with the specificity pocket of chymotrypsin positions the inactivator in such a way that attack of serine-195 occurs exclusively at the carbonyl carbon of **1**. No conjugate addition of serine-195 onto the halo-enol carbon of **1** is observed. Attack of serine-195 onto the carbonyl carbon of **1** leads to pyrone ring opening and hydrolysis of the halo-

enol-derived acid chloride to a carboxylate group. The carboxylate group forms a salt-bridge linkage to the protonated imidazole ring of histidine-57. This linkage precludes a water molecule from attacking the acyl linkage. Reactivation involves the reorientation of the terminal carboxylate group so that the salt bridge to histidine-57 is broken. The result is the rapid deacylation of the complex with the release of the isomerized (*E*)-4-benzyl-2-pentenedoic acid and native enzyme.

ACKNOWLEDGMENTS

We thank David R. Davies for a gift of γ-chymotrypsin crystals. We are grateful to Gregory A. Petsko for helpful discussions and for providing crystallographic facilities.

REFERENCES

Bernstein, F. C., Koetzle, T. F., Williams, G. J. B., Meyer, E. F., Jr., Brire, M. D., Rodgers, Y. R., Kenard, O., Shimanduchi, T., & Tasumi, M. (1977) *J. Mol. Biol. 112*, 535-542.

Cohen, G. H., Silverton, E. W., & Davies, D. R. (1981) *J. Mol. Biol. 148*, 449-479.

Gelb, M. H., & Abeles, R. H. (1984) *Biochemistry 23*, 6596-6604.

Henderson, R. (1970) *J. Mol. Biol. 54*, 341-354.

Hendrickson, W. A., & Konnert, J. H. (1980) in *Biomolecular Structure, Conformation, Function and Evolution* (Srinivason, R., Ed.) Vol. I, pp 43-57, Pergamon, New York.

Hummel, B. C. W. (1959) *Can. J. Biochem. Physiol. 37*, 1393-1399.

James, M. N. G., Sielecki, A. R., Brayer, G. D., Delbaere, L. T. J., & Bauer, C.-A. (1980) *J. Mol. Biol. 144*, 43-88.

Markley, J. L., & Ibanez, I. B. (1978) *Biochemistry 17*, 4627-4640.

Ringe, D., Petsko, G. A., Yamakura, F., Suzuki, K., & Ohmori, D. (1983) *Proc. Natl. Acad. Sci. U.S.A. 80*, 3879-3883.

Ringe, D., Seaton, B. A., Gelb, M. H., & Abeles, R. H. (1985) *Biochemistry 24*, 64-68.

Robertus, J. D., Alden, R. A., Birktoft, J. J., Kraut, J., Powers, J. C., & Wilcox, P. E. (1972) *Biochemistry 11*, 2439-2449.

Segal, D. M., Powers, J. C., Cohen, G. H., Davies, D. R., & Wilcox, P. E. (1971) *Biochemistry 10*, 3728-3738.

Sielecki, A. R., Hendrickson, W. A., Broughton, C. G., Delbaere, L. T. J., Brayer, G. D., & James, M. N. G. (1979) *J. Mol. Biol. 134*, 781-804.

Westkaemper, R. B., & Abeles, R. H. (1983) *Biochemistry 22*, 3256-3264.

NMR Study of the Molecular and Electronic Structure of the Heme Cavity of *Aplysia* Metmyoglobin. Resonance Assignments Based on Isotope Labeling and Proton Nuclear Overhauser Effect Measurements†

Usha Pande,‡ Gerd N. La Mar,*,‡ Juliette T. J. Lecomte,‡ Franca Ascoli,§ Maurizio Brunori,∥ Kevin M. Smith,‡ Ravindra K. Pandey,‡ Daniel W. Parish,‡ and V. Thanabal‡

Department of Chemistry, University of California, Davis, California 95616, Department of Experimental Medicine and Biochemical Sciences, University of Rome "Tor Vergata", 00173 Rome, Italy, and Department of Biochemical Sciences, CNR Center of Molecular Biology, University of Rome "La Sapienza", 00185 Rome, Italy

Received March 17, 1986; Revised Manuscript Received May 1, 1986

ABSTRACT: The ^{1}H NMR characteristics of the high-spin metmyoglobin from the mollusc *Aplysia limacina* have been investigated and compared with those of the myoglobin (Mb) from sperm whale. *Aplysia* metMb exhibits a normal acid ↔ alkaline transition with p$K \sim 7.8$. In the acidic form, the heme methyl and *meso* proton resonances have been assigned by ^{1}H NMR using samples reconstituted with selectively deuterated hemins and in the latter case by ^{2}H NMR as well. On the basis of the methyl peak intensities and shift pattern, heme rotational disorder could be established in *Aplysia* Mb; ~20% of the protein exhibits a reversed heme orientation compared to that found in single crystals. Three *meso* proton resonances have been detected in the upfield region between −16 and −35 ppm, showing that the chemical shift of such protons can serve as a diagnostic probe for a pentacoordinated active site in hemoproteins, as previously shown to be the case in model compounds. The temperature dependence of the chemical shift of the *meso* proton signals deviates strongly from the T^{-1} Curie behavior, reflecting the presence of a thermally accessible Kramers doublet with significant $S = {}^3/_2$ character. Nuclear Overhauser effect, NOE, measurements on *Aplysia* metMb have provided the assignment of individual heme α-propionate resonances and were used to infer spatial proximity among heme side chains. The hyperfine shift values for assigned resonances, the NOE connectivities, and the NOE magnitudes were combined to reach a qualitative picture of the rotational mobility and the orientation of the vinyl and propionate side chains of *Aplysia* metMb relative to sperm whale MbH_2O. Thus, it was found that the heme side chains are sterically less clamped in the former protein.

The myoglobin, Mb,[1] from the buccal muscle of the sea hare *Aplysia limacina* possesses several interesting properties that differentiate it from the more commonly studied mammalian Mbs. A number of structural and functional studies have

† This research was supported by Grants HL-16087 and HL-22252 from the National Institutes of Health and CU-84.01795.04 from the Consiglio Nazionale delle Ricerche.

‡ University of California.

§ University of Rome "Tor Vergata".

∥ University of Rome "La Sapienza".

[1] Abbreviations: Mb, myoglobin; metMb, metmyoglobin; Hb, hemoglobin; metHb, methemoglobin; NMR, nuclear magnetic resonance; NOE, nuclear Overhauser effect; Tris-HCl, tris(hydroxymethyl)aminomethane hydrochloride; Bis-Tris, 2-[bis(2-hydroxyethyl)amino]-2-(hydroxymethyl)-1,3-propanediol.

0006-2960/86/0425-5638$01.50/0